

Correlation between power density fluctuation and grain size distribution of laser annealed poly-crystalline silicon

Kenkichi Suzuki^a, Masakazu Saitou^a, Michiko Takahashi^a, Nobuaki Hayashi^a,
and Takao Terabayashi^b

^aElectron Tube & Devices Div., Hitachi, Ltd.

3300 Hayano, Mobara, Chiba 297 Japan

^bProduction Engineering Research Laboratory, Hitachi, Ltd.,

292 Yoshida-cho, Totsuka-ku, Yokohama 244 Japan

ABSTRACT

The grain size of polycrystalline silicon (p-Si) by the excimer laser annealing (ELA) is primarily determined by the fluence, and the distribution uniformity is strongly influenced by the intensity fluctuation. Instead of the conventional CCD profiler, an resist film is used to monitor the light intensity distributions over whole illumination area in submicron resolution. The high resolution measurements show speckle patterns with 0.1–0.15 μm spacing with maximum 10mJ/cm² variation. The fluctuation does not influence the grain size variation in the lateral growth region over 1–2 μm area, however, the undulation of intensity about 10mJ/cm² over 10 μm distance produces an appreciable changes in the grain sizes. Such a local temperature distribution corresponds to the envelop obtained by averaging small area, and is maintained during crystallization process.

Keywords: Polycrystalline silicon, Excimer laser annealing, Resist, Beam profiler.

1. INTRODUCTION

Many of the TFT-LCD manufacturers have launched production of the low temperature p-Si (LTP)TFT-LCD, as the performances of MOS transistors of p-Si become applicable to integration of the peripheral circuitries of some types of the displays. This is mainly due to qualities of ELA-p-Si¹⁾ and PE-CVD-SiO₂ which enable to realize usable TFT performances, e.g. the field effect mobility of more than several tens, sometimes 300 cm²/Vs in experimental level. The crystallinity of ELAp-Si has rather high quality inherent to liquid phase solidification, and the performances are considered to be degraded mainly by the grain boundaries. Larger grain size assures better performance. Actually a transistor with a single grain over 1 μm short channel shows more than 400 cm²/Vs. This stimulates developments of single crystallization techniques, and ultimately realization of a system-on-glass of high definition TFT-LCD, which is sole advantage of p-Si over the current a-Si TFT-LCD. There are so many experiments aiming larger grain sizes, new and mostly revised from '80s²⁾, however, they are a little far from practical applications because of lack of uniformity and reproducibility.

* Correspondence: E-mail: ksuzuki@cm.mobara.hitachi.co.jp; TEL: +81-475-25-9062; FAX: +81-475-24-2463

The uniformity and the reproducibility in the present LTP-TFT mass production is considered to be assured by smaller sized grains than a characteristic length, sacrificing higher performances. Typical characteristic length is usually a channel length (L), and is now $3\text{ }\mu\text{m}$ at most due to the current production equipments for large area substrates. So a reasonable grain size is no more than $0.3\text{ }\mu\text{m}$. This is primary condition of ELA process in manufacturing at present. The secondary condition comes from requirement from the device structure. The precursor film thickness should be less than 100nm , preferably near 50nm , as the LTP-TFT device is fundamentally SOI and the film thickness should be less than the depletion layer. The preferred film thickness is reasoned by less fluence resulting less throughput time and less production cost.

Thus the basic technology of ELA crystallization is to produce uniform and high graded p-Si film under these two conditions. For this purpose, it is essential to understand the mechanisms of ELA crystallization. More clearly we have to understand to what extent we can control the non-equilibrium phenomenon of ns time scale. From huge volume of the investigations hitherto, we can deduce some qualitative models for the grain growth, however, for mass production we need to know quantitatively what working parameters are effective and how they can be controlled. All these parameters seems to be classified into three categories; those related directly to ELA, the precursor film, and the interface. The first ELA parameters are fluence, shot numbers or repetition rate and the stage scanning speed, substrate temperature, atmosphere, and illumination uniformity. The second category includes film thickness, morphology and the concentration of hydrogen in the film. The third is difficult to define, but is related directly to crystallization dynamics, such as heterogeneous nucleation and lateral grain growth. At present the contributions of some of the parameters are considered to be almost established, however quantitative data necessary to the mass production are not necessarily sufficient, because the explicit technical parameters above are somehow coarse to control submicron grain growth. An example is CCD beam profiler, of which spatial resolution is usually $10\text{ }\mu\text{m}$ and monitors only confined region of the illumination area.

This paper presents a concept of the resist profiler which is possible to evaluate light intensity distribution over whole illumination area with submicron resolution. Such a profiler is essential because we are observing only intensity distribution in rather rough resolution at present although there may be microscopic fluctuations inherent to gas laser, and the grain size used is in submicron region. In the second chapter, the relationship between the ELA crystallization and the fluence and shot numbers are described according to our observations. The third chapter is devoted to the description of the technique of the resist profiler. The fourth and fifth are for discussions and conclusion.

2. FEATURES OF ELA POLYSILICON CRYSTALLIZATION

As a standard precursor Si film, we adopted a-Si film by LP-CVD of 50nm thick on quartz substrates. The deposition gas is monosilane (SiH_4) and the substrate temperature is $550\text{ }^\circ\text{C}$. ELA experiments are performed both by 248nm , $4 \times 8\text{ mm}^2$ and by 308nm , $0.3 \times 150\text{ mm}^2$ illumination area with nominal uniformity of $\pm 5\%$. The former is used mainly for examining the effects of temperature and atmosphere, and the latter is mainly for beam scanning.

The relationships between laser fluence and grain size are depicted in Fig. 1. The shot number is an fundamental factor for grain growth. One shot means solidification from precursor to polycrystalline, and the multi-shot corresponds to poly-to-poly transformation. The feature of grain growth is similar to both situations, that is, small grains at low fluence and

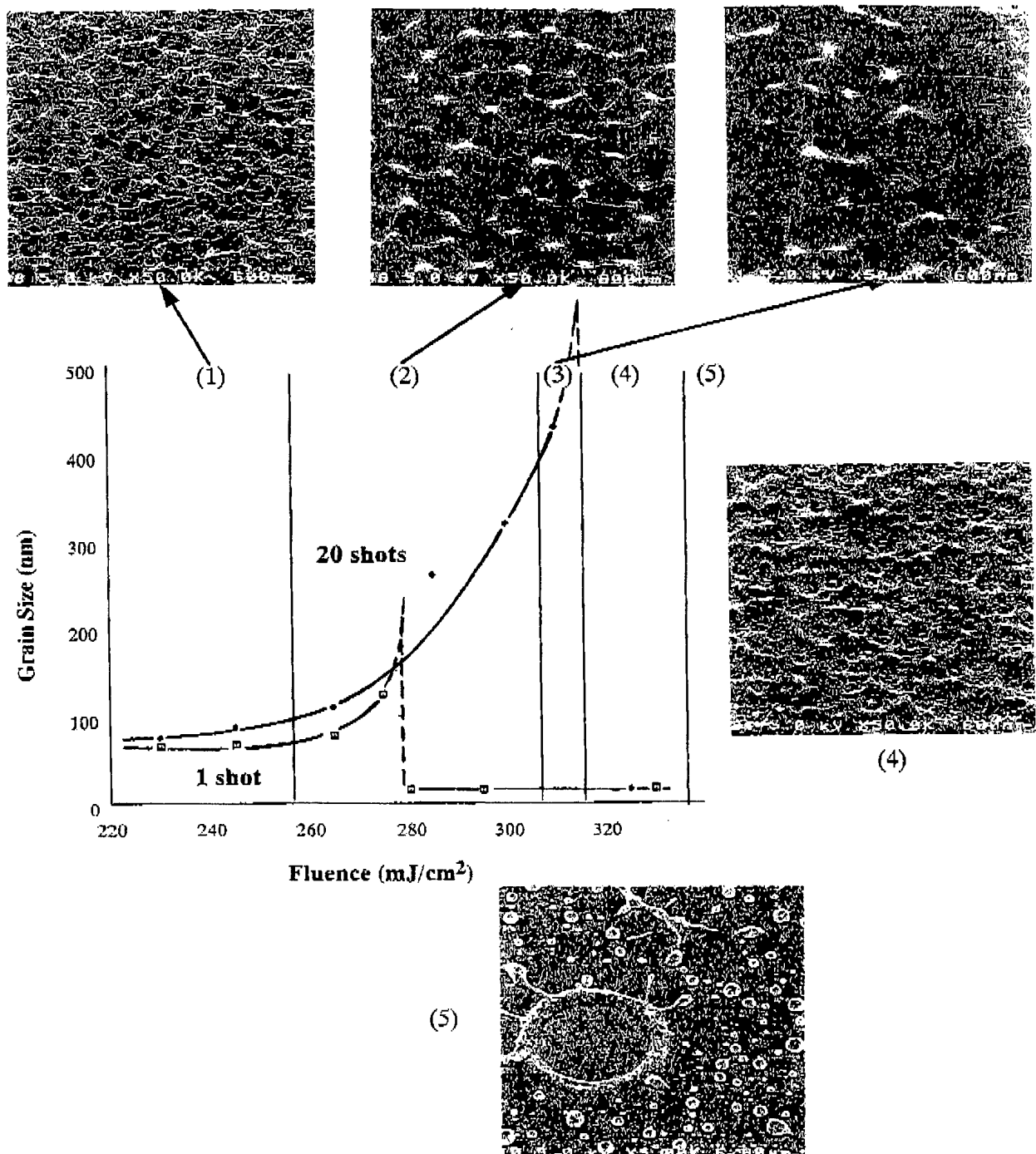


Fig.1 Relationship between fluence and grain size(average).

The grain growth is divided into 5 stages (here for 20 shots' case) , and the grains in each stage are shown in SEM picture.

becomes larger with fluence. The growth ends abruptly at a certain critical fluence, above which it becomes microcrystalline and amorphous mixture. Further increase of fluence results ablation. The fundamental difference between one- and multi-shot condition is the grain size and the uniformity of its distribution. The multi-shot grain size increases with shot number above a certain fluence, from which lateral growth starts. Improvement of the uniformity by the multi-shot seems to be also related to the lateral growth and is essential to practical applications. The grain growth is characterized by five stages according to the fluence, and SEM picture of typical grain structure at each stage is shown in Fig. 1. These pictures are results of 20 shots-LA in vacuum and at room temperature.

The first stage is vertical growth of small grains. When the size becomes nearly equal to the film thickness, the lateral growth is started. For 50nm film thickness, there is a particular size of the grain, approximately $0.3 \mu\text{m}$, which shows rather uniform distribution. This feature is very prominent when we use small pitch overlapping of scanning, e.g. $10 \mu\text{m}$, over wide area. The third stage is of rather larger grain size, but not uniform. It looks that the larger sized grains are constructed by merging smaller grains. The fluence of the abrupt transition to microcrystalline is different between one- and multi-shot, which is due to the differences of the melting point and the latent heat between amorphous and polycrystalline. The fourth stage is microcrystalline due to rapid bulk nucleation. The fifth is ablation. AFM data in Fig.2 show quantitative aspects of the grain growth. The bumps are created at the grain boundaries, and it is higher at a triple or sometimes quadruple junction. A grain corresponds to the valley between the peaks. The positions of the bottom of the valley, that is, the height of the grains, change randomly for the smaller grain region, but it becomes rather longer undulation when the grain size becomes larger.

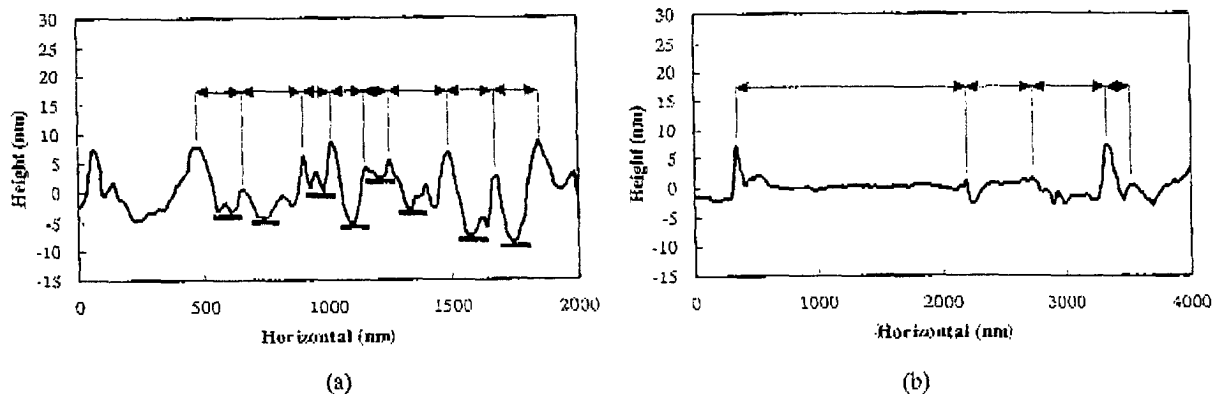


Fig. 2 AFM profiles of p-Si surfaces. (a) small grain size, (b) large grain size

The crystallization processes are qualitatively explained by a simple nucleation and crystal growth model, but the details are varied with different types of precursors. The most prominent is the onset fluence of ablation. This is apparently correlated to hydrogen contents in the case of amorphous Si by PE-CVD. The larger the hydrogen content, the smaller the ablation fluence. Sometimes the film is ablated without the pass of microcrystalline phase. The PE-CVD precursors are mostly amorphous, and the morphology is strongly influenced by H contents, making various types of Si-H bonds³⁾. The various bonding structure makes it difficult to dehydrogenate completely, and results fluctuation in crystallization process. Even the

films by sputtering sometimes show very low ablation threshold, although H concentration is very low. It seems that morphology, microcrystallinity or defects, irrelevant to H are also the cause of such a behaviour. Higher substrate temperature results lower fluence to make same supercooling than r.t., and sometimes it improves the uniformity.

3. RESIST BEAM PROFILER

The most common beam profiler makes use of CCD camera. The pixel size is $5\text{ }\mu\text{m}$ square in minimum, and the number of pixel is 1M (XGA) usually. Accordingly with 1:1 image system, the resolution is just $5\text{ }\mu\text{m}$. It is improved by a magnified optics. A conventional magnifier is the objective lens of the microscope, and we can obtain ideally $0.2\text{ }\mu\text{m}$ resolution with an adequate optics($\times 100$) corresponding to a CCD pixel at minimum resolution. The drawback is reduction of the objective field. In the case of the highest resolution above it is $0.2\text{mm}\phi$. The field spreads upto $1.0\text{mm}\phi$ when $\times 20$ objective lens is used. However the resolution is reduced to $0.5\text{ }\mu\text{m}$.

Our objective is to measure the intensity distribution with submicron resolution over all beam area. Only resist film can realize such a high spatial resolution over wide area. The principle of the resist beam profiler is very simple. The light incident into a resist film react with the material, producing insoluble or soluble region according to the types of resists, proportional to light intensity. The following development process removes or fixes the reacted region, and the light intensity is mapped as surface undulation. The configuration of the resist profiler system is shown schematically in Fig. 3(a). The homogenized beam is splitted by the mirror, and illuminates the resist film through a conjugate optics. The resist film is moved by X-Y stage to be exposed with each shot. The surface profiles are measured by various types of high resolution profilers and by AFM. Resist sensitivity should be linear in low light intensity. There must be a base plane flat

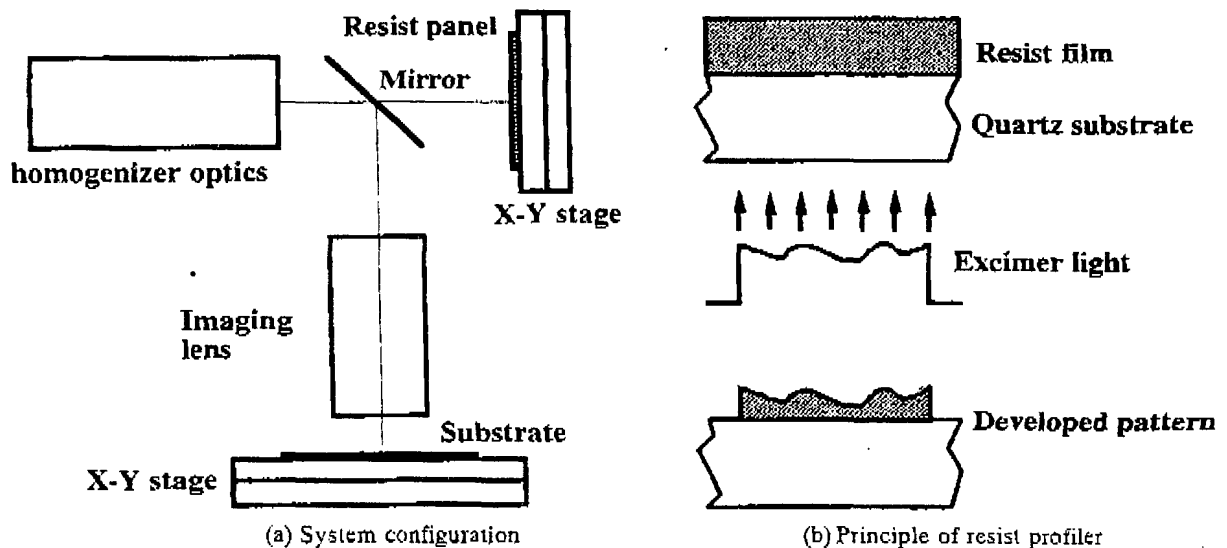


Fig. 3 Resist profiler system

enough to measure the roughness produced by light intensity distribution. Such a flat basis is obtained only by a substrate surface. It follows that the light should be illuminated from the substrate side, and thus to use a negative type resist film as shown in Fig. 3(b). This configuration prevents also LIPSS structure⁴⁾.

Phenol-azido system⁵⁾ is selected as resist material. The matrix resin is poly(p-vinylphenol), and the chromophore is 3-3'-diazidodiphenyl sulfone. This material was synthesized originally for the resist sensitive to ultraviolet region. The photochemical reaction scheme is depicted in Fig. 4. Ultraviolet light activates azido radicals of the chromophores, which subsequently release nitrogen, and are changed to an intermediate nitrene. The nitrenes extract hydrogens at aryl-carbons in the resin monomers, which are polymerized and become insoluble. The sensitivity and linearity is controlled by the concentration of the chromophore and the molecular weight of the matrix.

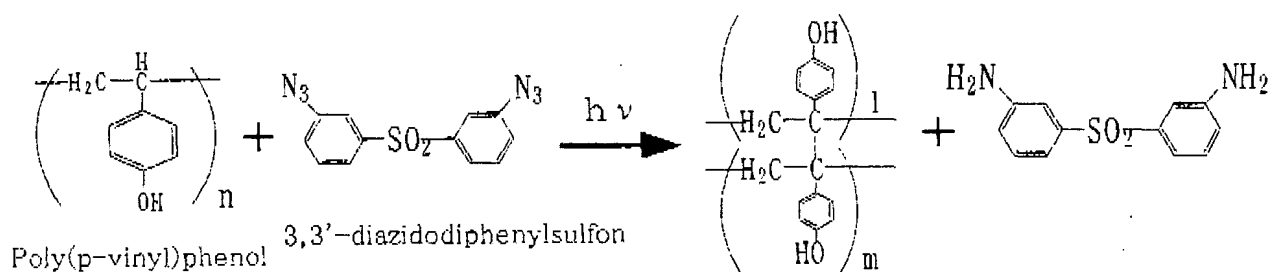


Fig. 4 Photochemical reaction scheme of the resist

The relationship between fluence (1 shot) and developed film thickness is shown in Fig. 5. The dynamic range (defined by the ratio of average film thickness after development and minimum variation from the average) is conditioned by the concentration of the developer chemicals and developing time. The resist film is coated on a quartz plate, and baked 1 hour at 100°C. The light is illuminated from the rear of the plate and developed. An average film thickness is measured by a profiler (DEKTAK) and the surface undulation is measured by an optical type of profiler (Wyko TOPO-3D) and AFM. The flatness of the substrate surface is finished to $\lambda/10$, and the R_a of the substrate surface is less than 0.15 nm for $2 \mu\text{m}$. This value assures the accuracy to measure the local variation of the resist surface.

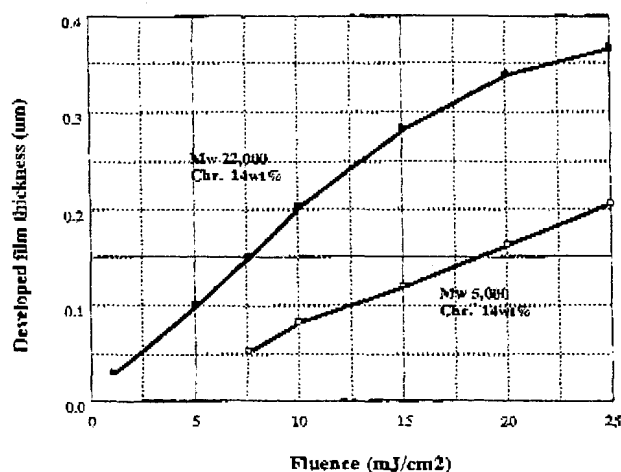


Fig. 5 γ -characteristics of the resist

The sensitivity is strongly dependent upon molecular weight, rather than the concentration of the chromophore.

4. RESULTS AND DISCUSSIONS

Comparison between the profiler(WYKO) picture and p-Si micrograph (Nomarski) is shown in Fig. 6. To distinguish the variations of illumination, a little deteriorated homogenizer optics are used. The spatial resolution of the profiler(WYKO) is $0.5 \mu\text{m}$. The measurement area is $1\text{mm} \times 1\text{mm}$, a part of whole illumination region $4 \times 8 \text{mm}$. The average film thickness is approximately 300nm , and is corresponding to 180 scales. The variations are ± 38 scales. From Fig.5 and taking into account of 20:1 attenuation of the intensity on the resist film, the profiler maps about $\pm 20 \text{ mJ/cm}^2$ variation of the light intensity.

The Nomarski micrograph of Fig. 6(b) is corresponding to the same area of p-Si surface, obtained by 10 shots. The change of the intensity distribution at each shot supposed to be small owing to the homogenizer optics. The colours in the micrograph come from Rayleigh scattering by the roughness due to the bumps on the surface. The averaged height of the bumps is proportional to the grain size, and thus the colours represent the grain sizes; black at starting amorphous, pale green at small grains, green at $0.1\text{--}0.3 \mu\text{m}$, blue at $0.3\text{--}0.5 \mu\text{m}$, white at more than $0.5 \mu\text{m}$, and again black at microcrystalline. There is no one-to-one correspondence between details in two pictures, because the relationship between fluence and the grain size is not similar to the relationship between colour and the grain size. However there are close resemblance between two figures. It should be also noticed that the resolution is limited by the measurement method and instrument. As the whole profile of the illumination region is mapped on the resist profiler, there are two possibilities to utilize the profile data; improvement of homogenizer optics by rather coarse resolution, and the analyses of local grain growth mechanisms by fine resolution.

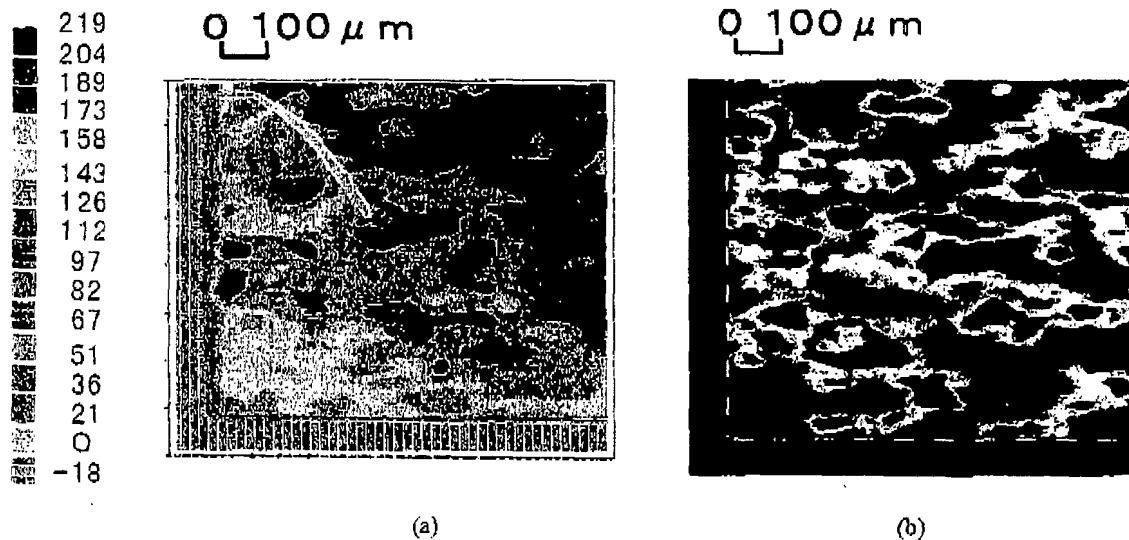


Fig. 6 Comparison between the profiler chart of the resist (a) and Nomarski micrograph of p-Si (b)

The base of the resist profiler is a gamma characteristics, which is the relationship between fluence and developed film thickness. The absolute resolution is defined as minimum thickness or volume removed by development for minimum light exposure (in the case of negative resist). Experimentally it is very difficult to define minimum light intensity, as the fluence of the excimer laser changes more than $\pm 10\%$ shot by shot. Besides, the profile is not always uniform due mainly to homogenizer optics. Each point on the gamma curve in Fig. 5 is an average determined from measurements of the thickness of ten one-shot profiles for each nominal fluence by the profiler (Wyko) at the same point. The minimum resolution is inferred from comparison among ten profiles. It is 3nm for $0.2\text{mJ}/\text{cm}^2$ at averaged total thickness 300nm for $15\text{mJ}/\text{cm}^2$. The rms roughness of the substrate surface is less than 0.15nm over $2\text{ }\mu\text{m}$, which is far less than minimum resolution of the resist. As stated previously monitoring light is reduced to 1:20. Accordingly at $300\text{mJ}/\text{cm}^2$ illumination to a sample, $\pm 2\text{mJ}/\text{cm}^2$ variation can be detected. The absorption coefficient of the resist is $2.2 \times 10^4\text{cm}^{-1}$ at 248nm . This value does not change appreciably with the concentration of the chromophore. The developed film thickness is 300nm in average, and up to the thickness from the substrate, the exponential decay curve of the intensity is well approximated to be linear. This means there is no truncation in the details of the profile. The result of higher resolution measurement by AFM is shown in Fig. 7. The speckle pattern is clearly recognized. The high spots in the speckle are about 10nm at most, that is, $10\text{mJ}/\text{cm}^2$. Although almost all the values are near to the resolution limit and not so accurate, there are intensity fluctuations with nearly half wave length period over whole illumination area.

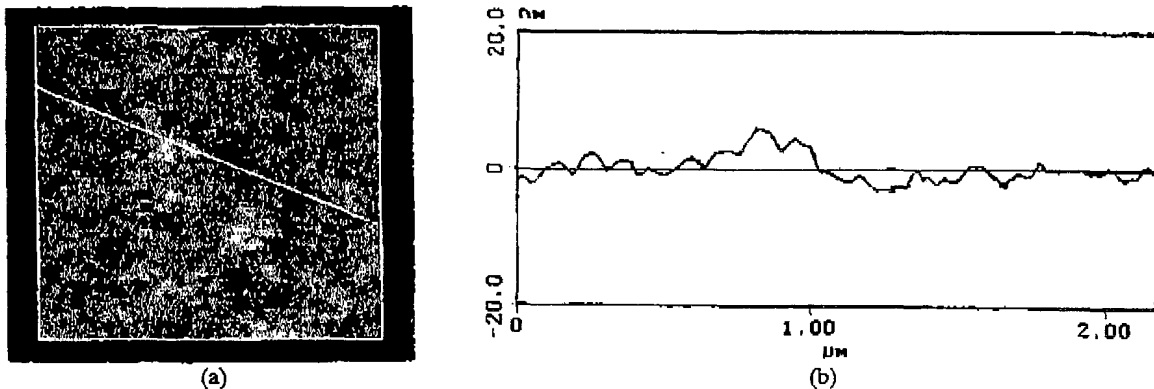


Fig. 7 AFM picture of the resist surface. (a) speckle patterns, (b) scanning chart

From Fig. 1 it is pointed out that the variation $10\text{mJ}/\text{cm}^2$ produces about two times differences of the grain size at $0.3\text{ }\mu\text{m}$ region. However SEM pictures show that the distribution of the grain size does not vary appreciably over $1\text{--}2\text{ }\mu\text{m}$ area, although the speckle spacing are $1/10$ of the region and the lateral grain growth is considered to start from $0.05\text{ }\mu\text{m}$. Such uniformity is enhanced when shot number is increased, and it is most prominent at $0.3\text{ }\mu\text{m}$ region. This suggest some factors other than fluence are equally essential for the grain growth. Multi-shot ELA is a process of repetition of melt and recrystallization. In the course of the repetition, smaller grains tend to disappear, as they are melted faster than the larger owing to the ratio of boundary area and volume. There is higher probability that a nucleation appears at the larger grain site. Repetition seems to multiply the probabilities. However intensity variation about $10\text{mJ}/\text{cm}^2$ over more than $10\text{ }\mu\text{m}$ area

is clearly observable as the change of the grain size. The larger distance variation is effectively an envelop of the intensity distribution averaged over $1\sim 2\ \mu\text{m}$ area. From observations of optical micrographs (Nomarski) of p-Si surface, it is reasonable to assume that the pattern of the averaged distribution is maintained during the crystallization period. The grain distribution is regarded to be preserved even during multi-shot illuminations. The localization of temperature distribution during crystallization period is prominently exhibited in the SEM picture in Fig. 8 of the region where area of the larger grains are adjacent to the microcrystalline region.

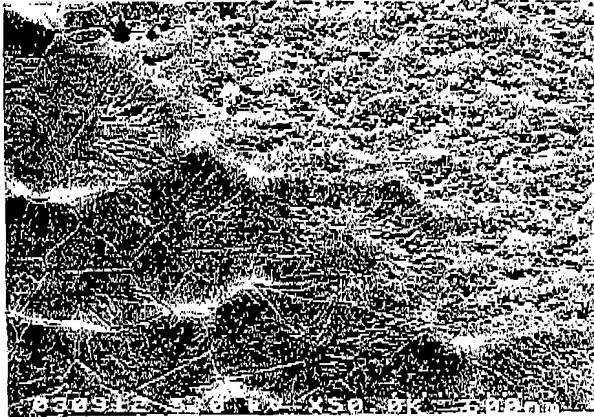


Fig. 8 SEM picture of the boundary between large grain region and microcrystalline region

Smearing out of light intensity fluctuation over $1\sim 2\ \mu\text{m}$ area is explained by thermal diffusion length $\sqrt{2Dt}$ in the liquid phase of Si film. D is thermal diffusion coefficient, and t is a full pulse duration. In the liquid phase, D is $0.07\ \text{cm}^2/\text{s}$, and the diffusion length is $0.8\ \mu\text{m}$ for $50\ \text{ns}$ full pulse duration. It is inferred that the lateral growth is confined within the locally uniform temperature region. The duration staying in liquid phase is approximately proportional to the incident fluence. Accordingly the smearing area will be proportional to square root of the fluence. However the grain size increases much faster as shown in Fig. 1. It is evident that the large sized grain is resulted by lateral grain growth, and larger grain is obtained by faster lateral motion. According to the theory of the interface response function⁷⁾, there is a maximum at a certain supercooling. The supercooling in our experimental conditions always exists at the lower side of the maximum, as the higher fluence produces the larger grains as shown in Fig. 1. Over the maximum toward higher temperature, it does not result any reduction of the interface velocity but bulk nucleation producing microcrystalline. This may be a characteristic feature of the heterogeneous nucleation and thin film.

The bumps at the grains is another feature to be elucidated. It is an important phenomenon to understand the mechanisms of grain growth, and at the same time, it is very obstructive structure for TFT performances and is needed to be reduced. This structure suggests an upheaval of viscous liquid thrust between solid plates. This leads a simple model; a nucleus is created at the centre of locally uniform temperature region, and it grows initially vertically and next laterally. If there are such nuclei situated at equidistance and grow equally, then they collide side by side and at junction according to the growing crystallographic axis. The middle part of the grains stays liquid, as the latent heat is released. The exothermic process also prevent small grain growth according to the velocity of the interface.

5. CONCLUSION

The resist beam profiler can map whole illumination area with high resolution. The effective resolution is limited by the resolution power of measurement equipments. High resolution measurements reveal existence of speckle patterns with 0.1-0.15 μ m spacing. The fluctuation over 1-2 μ m area does not influence the grain growth. On the other hand, the undulation of temperature distribution over 10 μ m area obtained by averaging the small scale fluctuation maintains its distribution pattern during crystallization period, and thus it determines the grain sizes and the distribution. The localization of intensity envelop is on the one hand owing to the homogenizer optics which reduce spatial variations of the beam profile if it does not change substantially. On the other hand, it suggests that cooling speed and resulting nucleation is much higher than the lateral thermal diffusion time, as is pointed out by many investigations. Accordingly accurate design of the homogenizer optics and control of cooling process through the buffer layer and the substrate over 10 μ m area is essential to realize uniform grain distribution. The resist beam profiler gives quantitative data necessary for the purpose.

REFERENCES

1. T. Sameshima et al., *IEEE EDL* **7** (1986) 276 ; H. Kuriyama et al., *Jpn. J. Appl. Phys.* **31** (1992) 4550
H. Kuriyama et al., *Jpn. J. Appl. Phys.* **32** (1993) 6190
2. E.I. Givargizov, "Oriented Crystallization on Amorphous Substrates", Plenum Press, New York (1991)
H. Kuriyama et al., *Jpn. J. Appl. Phys.* **30** (1990) 3700 ; H. Kuriyama et al., *MRS Symp. Proc.* **321** (1993) 657
K. Shimizu et al., *IEEE T-ED* **40** (1993) 112 ; D.H. Choi et al., *Jpn. J. Appl. Phys.* **33** (1994) 70 ; R. Ishihara et al., *Jpn. J. Appl. Phys.* **34** (1995) 1759 ; R. Ishihara et al., *Elect. Lett.* **31** (1995) 1956 ; J.S. Im et al., *MRS Bulletin* vol 21 [3] (1996) 39 ; K. Ishikawa et al., *Jpn. J. Appl. Phys.* **37** (1998) 731
3. M.H. Brodsky, "Properties of Amorphous Silicon", Chapter 2 in "emis data review series #1", ed. by J.M.D. Thomas INSPEC (1985) ; R.A. Street, "Hydrogenated Amorphous Silicon", pp44 - 61, Cambridge Univ. Press (1991) ;
E.A. Davis, *J. non-Crystall. Solids*, **198 - 200** (1996) 1 ; C.G. van de Walle, *ibid.* **227 - 230** (1998) 111
4. S.E. Clark and D.C. Emmony, *Phys. Rev. B* **40** (1989) 2031
5. T. Iwayanagi, et.al., *IEEE Trans. Electron Devices*, **ED-28** (1976) 1306 ; T. Iwayanagi, et.al., *J. Electrochem. Soc.*, **127** (1980) 2759
6. A. Goldsmith, "Handbook of Thermodynamic Properties of Solid Materials", MacMillan, New York (1961)
7. D. Turnbull, *J. Phys. Chem.* **66** (1962) 609 ; M.D. Kluge and J.R. Ray, *Phys. Rev. B* **39** (1989) 1738 ;
S.R. Stiffler et al., *Acta Metall. Mater.* **40** (1992) 1617